

**REPLACE THIS PAGE WITH A SCANNED
COPY OF YOUR OFFICIAL, SIGNED
DISSERTATION ACCEPTANCE FORM (DAC)**

Page left intentionally blank.

Thesis Title Goes Here

A dissertation presented

by

Soumya Roy

to

The

in partial fulfillment of the requirements

for the degree of

Doctor of Philosophy

in the subject of

The Inter-University Center for Astronomy and Astrophysics

Pune, India

Month Year

Dissertation Advisor: Professor Durgesh Tripathi

Soumya Roy

Thesis Title Goes Here

Abstract

An ABSTRACT goes here.

Contents

Abstract	ii
Acknowledgments	iv
Dedication	v
1 Introduction	1
1.1 The solar interior	1
1.2 The solar atmosphere	2
1.2.1 The Photosphere	3
1.2.2 The Chromosphere	4
1.2.3 The Transition Region	5
1.2.4 The Corona	5
1.3 Solar Flares	6
1.3.1 Brief history of flare observation	6
1.3.2 Neupert effect	8
1.3.3 Standard model of solar flare	8
1.3.4 The energetics of solar flares	10
1.4 Motivation	11
1.5 Outline of Thesis	11
2 Existing Solar Observations and techniques	13

CONTENTS

2.1	Introduction	13
2.2	The Aditya-L1	13
2.3	The Solar Ultraviolet Imaging Telescope	13
2.3.1	SUIT & Solar Flares	13
3	Intital preparatory analysis for SUIT	19
3.1	Introduction	19
3.2	Throughput model of SUIT	19
3.3	Filter Choice for SUIT	19
3.4	Photometric, Radiometric & Spectral Calibration of SUIT	19
4	Forward modelling SUIT observations	21
5	Stellar calibration of SUIT	23
6	Effects of Solar flares on the local plasma environment from Mg II observations	25
6.1	Introduction	25
7	Estimating thermal and non-thermal energy partition of Solar Flares	29
8	First X-class flare observed from SUIT	31

Acknowledgments

Thank people here.

Your thoughtful dedication goes here.

Chapter 1

Introduction

The Sun is our nearest astrophysical object, which serves as a natural laboratory for various branches of Physics - atomic physics, spectroscopy, turbulence, magnetohydrodynamics, stellar evolution, dynamo and magnetism and plays a key role in space and terrestrial weather. The Sun is also the primary source of light and energy on earth. So it is only natural that we try to understand the different physical processes involved in the energetics of the Sun, which indirectly affects life on Earth. In this chapter I briefly introduce the Sun and various layers of its atmosphere. At the end we provide a motivation for the thesis.

The Sun is a G2V star, with surface luminosity 3.86×10^{26} W and an effective temperature of ~ 5780 K. The Sun is mostly made out of Hydrogen(92.1%) and Helium(7.8%) along with negligible quantities of heavier elements C, N, O, Mg, Si, Ne and Fe. The study of the Sun can be mainly divided into three components: the Solar interior, the Solar atmosphere and the Heliosphere.

1.1 The solar interior

In the innermost zone of the star the Sun has a temperature of about 15 MK and a density of 1.6×10^5 km.m⁻³ that fuses Hydrogen into Helium mainly by p-p cycle and to some extent by CNO cycle [SR: Ref here].

Fig. 1.1 shows a schematic diagram of various layers of the Sun. Beyond the core we have the optically thick radiative zone, where the Hydrogen and Helium are completely ionized [SR: Ref. here]. The high energy γ -ray photons generated in the core, have very small mean free path in this region, as they collide numerous

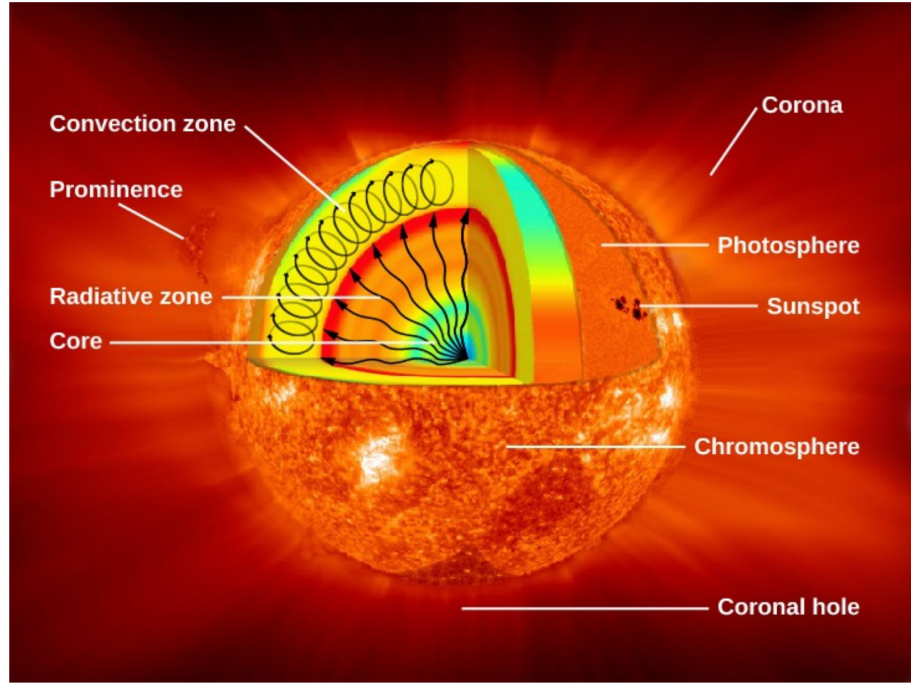


Figure 1.1: A schematic depiction of the different layers of the Sun. The figure also shows some of the most prominent magnetic structures on the Sun e.g sunspot, prominence, coronal hole. Credit : NASA/Goddard. [SR: Better pic here.]

times eventually thermalizing becoming visible photon. Beyond the radiative zone the degree of ionization of Hydrogen and Helium changes drastically giving rise to a sharp temperature gradient. This is the convective zone where the energy from the inner layers of the Sun is transported adiabatically to the surface of the Sun. In between the radiative and the convective zone, there is a thin layer, roughly at $\sim 0.7 R_{\odot}$ known as the tacholine, which is believed to play a major role in generating Sun's magnetic field via the Dynamo process [SR: Ref. here].

The core and the radiative zone of the Sun rotates as a solid body, whereas the convective zone rotates differentially. The rotation period varies from ~ 25 days to ~ 35 days from the equator to the pole.

1.2 The solar atmosphere

The layers outside the convection zone together, form the solar atmosphere - the Photosphere, which is also known as the Sun's surface, the Chromosphere, the transition region and the Corona. While we can define geometrical height or depths

CHAPTER 1. INTRODUCTION

to define these layers, it is much more useful to define them using the local optical depths of various spectral lines, which are directly used to observe the layers. This also gives us an idea about which spectral features originate mainly from which portions of the solar atmosphere. Fig. 1.2 shows the variation of temperature and number density across various layers of the Solar atmosphere [SR: Ref. here].

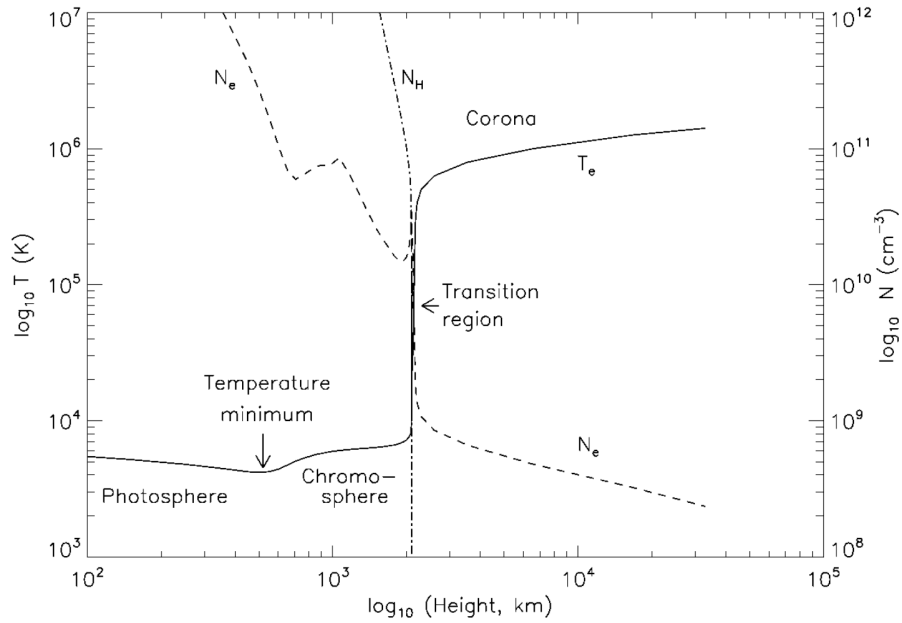


Figure 1.2: The variation of electron temperature (solid line) and electron density (N_e , dashed line) and density of neutral hydrogen atoms (N_H , dotted-dashed line) in the solar atmosphere as derived based on the 1-D model calculations by [SR: Ref. here].

1.2.1 The Photosphere

The Photosphere is defined to be the layer where $\tau_\lambda \sim 5000 = 1$. This is in the green part of the visible spectrum and the Sun is opaque in visible beyond this layer, hence it is called to be the surface of the Sun. This layer is 400-600 km deep and has an effective temperature of 5780 K. The magnetic field lines arising from the tacholine penetrate the Photosphere and creates a ‘carpet’ over the whole region [SR: (Priest 2014) ref here]. As mentioned earlier, this is the Solar surface known as the ‘Quite Sun’(QS from hereon). This region exhibits an average magnetic flux density of **10 – 50 G**. The QS surface is covered with cells of roughly four size- granule, meso granules, super granules and giant cells. Some regions exhibit much stronger

CHAPTER 1. INTRODUCTION

magnetic flux density often associated with highly twisted magnetic field structures. These magnetic features are manifested as sunspots, spicules, bright points etc.

As the density changes drastically at the Photosphere compared to the convective zone, the thermalized photons from Sun's core start free streaming again, as the mean free path also increases drastically and as a result perturbs the thermal equilibrium (TE from hereon). So, we have to define the thermodynamic quantities of the Photosphere in Local Thermal Equilibrium (LTE from hereon). As we move away from the Photosphere, because the density keeps on decreasing steadily, the LTE conditions also start deviating similarly [SR: [Ref here](#)].

1.2.2 The Chromosphere

The Chromosphere is a highly non-uniform dynamic layer with a thickness of 1500 – 3000 km, with increasing temperature (upto 10^4 K) and decreasing number density. As seen in the fig. 1.2, the temperature of the Chromosphere saturates before the dramatic rise in the transition region. This saturation is attributed to a steady deposition of acoustic energy by creation of shock waves [SR: [Ref. here](#)]. The Chromosphere also exhibits a sharp gradient in the plasma β factor, non-LTE conditions, dominance of wave motions [SR: [Ref. here](#)].

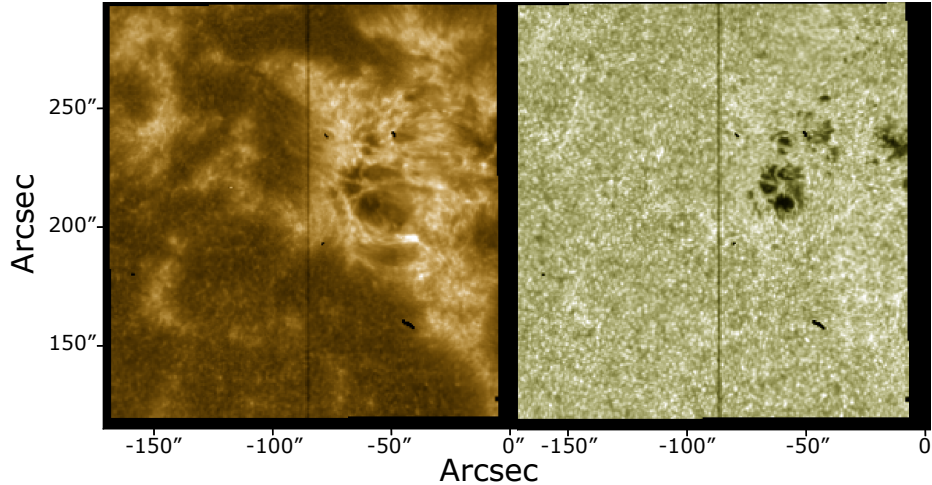


Figure 1.3: IRIS SJI Slit-jaw images of NOAA AR 13521 on Dec 21st, 2023 in Mg II 2796 Å (left panel) showing the upper Chromosphere. The right panel shows the same active region in 2832 Å continuum corresponding to upper photosphere.

In fig. 1.3 we show the NOAA AR 13521 in IRIS SJI 2796 Å(left panel) and 2832 Å(right panel). The dark sunspots and plage regions surrounding it are clearly

CHAPTER 1. INTRODUCTION

visible in the 2832 Å wavelength window. In the 2796 Å window we see the plage along with light bridges more clearly.

1.2.3 The Transition Region

The transition region above the Chromosphere is a thin, dynamic layer where we witness a dramatic increase in temperature by two orders of magnitude along with a similar decrease in electron density by nearly 5-6 orders of magnitude which is demonstrated in fig. 1.2. In general the this layer is roughly ~ 100 km in thickness, but that can change depending on various dynamic conditions of Chromosphere($\sim 10^4$ K) below, or Corona($\sim 10^6$ K) on top. The transition region is generally characterized by the steep change in the temperature, pressure gradients, drastic change in local optical depth and competition between gas pressure and magnetic pressure. The transition region also manifests the ARs as various magnetic features such as small scale brightenings, jets, spicules, fibrils etc.

1.2.4 The Corona

The outermost layer of the Solar atmosphere is the Corona. The Corona is only visible in naked eyes during the total solar eclipse or via Coronagraphs. It maintains a steady temperature of 1-2 Mk during ambient conditions, but can rise upto tens of MK during solar flares. The coronal continuum spectrum is produced due to Thompson scattering of photons from photosphere off coronal electrons. Corona also emits in various emission lines, e.g. Mg, Fe, Si, S, Ca, O etc. across a wide band of electro magnetic spectrum ranging from X-ray to visible wavelengths.

Similar to the other layers, the corona exhibits a variety of structures such as ARs, coronal holes, bright points, filaments, flares. The flare arcades are most prominently visible in the Corona. So, most of our existing studies over the last decade has focused on the coronal features of the flares. In fig. 1.3 we show one of the most well known and well studied solar eruptions from Aug 31st, 2012. A giant prominence erupted from the south east limb. The erupted prominence material was visible in all AIA channels from 304 Å (Chromospheric He II, see fig. 1.4 **panel (a)**) across all six Coronal channels (**panel (b)-(g)**). The sun spots were also clearly visible in HMI magnetogram and continuum (see fig. 1.4 **panel (h)**). In **panel (i)** we show the co-aligned AIA 304 Å, 131 Å and HMI magnetogram image. The sunspots lie at the base of the erupted prominence, accompanied by the hot thermal plasma associated with the accompanying flare. The novelty of such observation lies

CHAPTER 1. INTRODUCTION

in the clear spatial connection across various layers of the sun, connected via energy and momentum transported from one layer to the other.

1.3 Solar Flares

Solar flares are the most powerful magnetic events in the solar system. They are described as a sudden increase in brightness in localized areas on Sun. Within tens of minutes, they can release over 10^{32} erg of energy, which is emitted across the entire electromagnetic spectrum from radio to gamma rays. They can also launch high energetic particles into the interplanetary medium. Most of the flares occur in magnetic active regions, and the amount of flare energy released is comparable to the free energy stored in the magnetic system. The term "flare" is generally used explicitly for the entire magnetically-driven event's electromagnetic radiation, as it is the most significant fraction of the total energy liberated. The total energy released varies from event to event. It is also known that larger events occur much less frequently than smaller events.

1.3.1 Brief history of flare observation

In September 1, 1859, R.C. Carrington and R. Hodgson observed the first flare in the continuum of white light(??). The localized brightenings on the Sun have remained an enigma ever since. We have been observing the local flaring events across all wavelengths from both ground and space based observatories. Shortly after the observation by Carrington and Hodgson, people started studying the Sun extensively in the H α line which is formed in the Chromosphere, and the reports of flaring events became more and more frequent and progressively more and more complex. No two events were similar, as there were variations observed in source of size, ejections of plasma along with shockwaves driving into the interplanetary space. Advances of radio technology during the second world war ensured detections of presence of non-thermal electrons in the solar corona, during military radar operations (?). Around the same time S.E. Forbush noticed ground level cosmic ray enhancement during major solar flares. These discoveries illuded that the flaring events do not only involve the thermal plasma, but is somehow connects with high energy particles and involves the corona. in the 1950s we started observing the Sun in hard X-rays (≥ 10 keV) with rockets and balloons. ? discovered the first hard X-ray emission during a flare in 1958. Later on, it was deduced from the observations of the enhancements observed in radio and hard X-rays that, the the

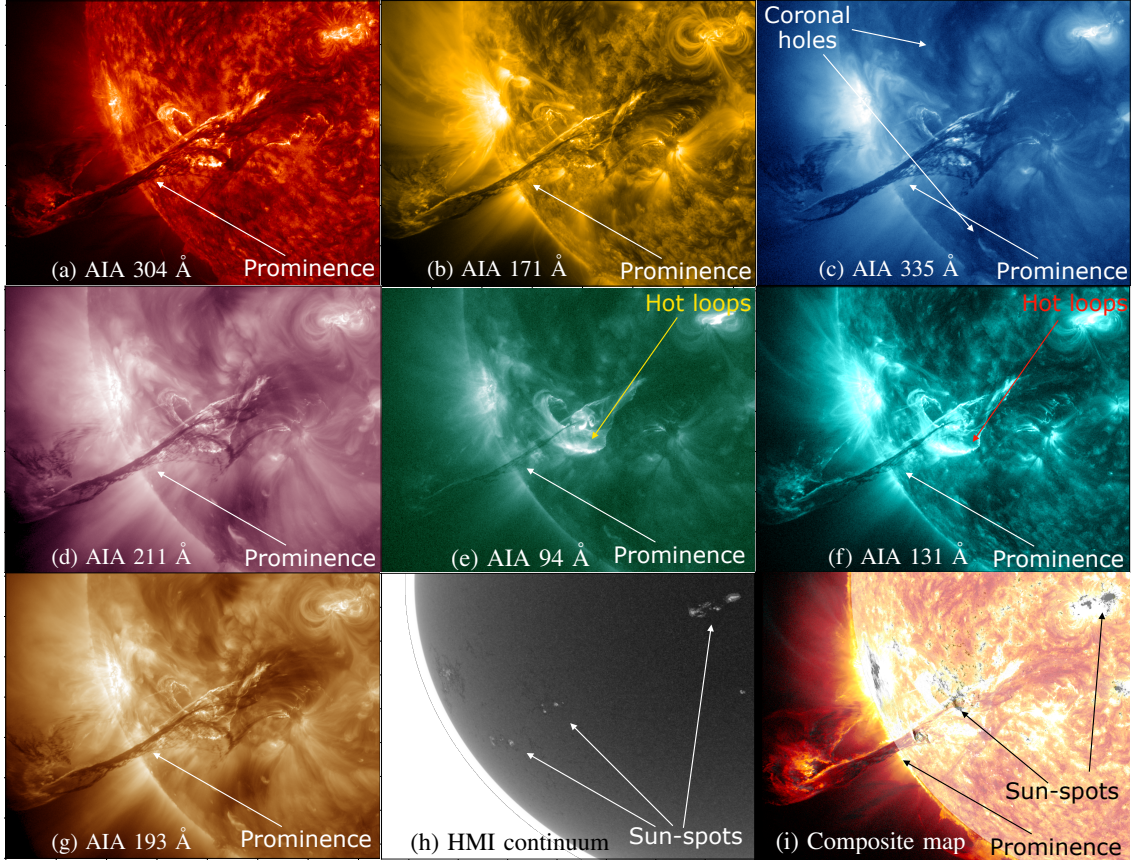


Figure 1.4: Image of the prominence eruption and associated flare from NOAA AR 11562 on Aug 31st, 2012~19:50 UT. The prominence is visible in all of the AIA channels. We see the coronal holes in AIA 335 Å (**panel c**). The flare loops of the associated event is visible in AIA 94 Å (**panel e**) and AIA 131 Å (**panel f**). The sunspots are visible in HMI continuum **panel (h)**. We show a co aligned map of AIA 304 Å, HMI magnetogram and AIA 131 Å in **panel (i)**. The spatial association of the sunspots with the hot flareloop plasma and the prominence eruption is clearly demonstrated here.

CHAPTER 1. INTRODUCTION

ejected energetic particles may contain a substantial fraction of the initial energy released (?). The hard X-ray is created by the bremsstrahlung of the electrons colliding into dense material, resulting in a power-law energy distribution. The broadband radio emission from 1 to 100 GHz is created from gyrosynchrotron emission. Finally, observations in EUV and soft X-ray (≤ 10 keV) have shown that the energy released from the flare heats the plasma contained in the coronal loops to temperatures beyond 30 MK.

1.3.2 Neupert effect

? observed a curious correlation that, the soft X-ray flux during the rise phase of the flare is proportional to the time integral of the centimeter radio flux since the start of the flare. The centimeter radio flux is emitted by relativistic electrons. So, later on the same correlation was found between the hard X-ray flux and soft X-ray flux and can be expressed as,

$$F_{SXR}(t) \propto \int_{t_0}^t F_{HXR}(t') dt' \quad (1.1)$$

This empirical relation is known as the “Neupert effect”. ? had already suggested that this may be due to a causal relationship between the thermal plasma and the energetic electrons. The logical explanation is: the soft X-ray mainly originates from a thermal plasma heated by the energy of the flaring event deposited by the flare accelerated electrons. It is important to mention that we know now, eqn.1.1 is only valid if cooling by conduction of radiation is negligible.

1.3.3 Standard model of solar flare

There were several observations like Neupert effect, which would help us to constrain several phenomenon observed in the flares:

1. The magnetic reconnection happens in corona, releasing the magnetic free energy. Electrons and energetic particles from the reconnection site are accelerated along the realigned magnetic field lines. The accelerated particles that escape along the open field lines towards the earth gives rise to the particle events seen from earth.

CHAPTER 1. INTRODUCTION

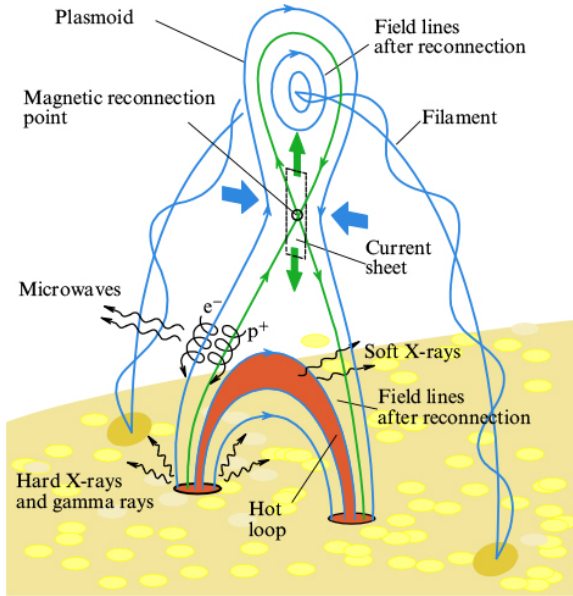


Figure 1.5: A schematic diagram of the standard model of solar flare.

2. The accelerated particles move along the field lines downwards along the magnetic field lines, giving rise to the microwave observations seen from flares via gyromagnetic radiation.
3. The accelerated particles hit the Chromosphere which is considerably denser than the Corona, giving rise to Hard X-ray and gamma ray observed from the footpoints. This also explains why the coronal hard X-ray source is considerably softer than the footpoints. The energetic particles deposit their energy into the local Chromosphere, as they go through series of collision and eventually thermalize.
4. As the plasma thermalizes, it starts emitting in thermal bremsstrahlung giving rise to the soft X-ray observed. Also, as the energy is deposited into the Chromosphere from the accelerated particles, it heats the local Chromosphere environment it gradually increases the local pressure.
5. As the pressure grows, when the pressure gradient builds up enough the local plasma starts expanding upwards(essentially due to buoyancy) and slowly fills up the coronal loops with soft X-ray emitting plasma. This phenomenon is known as "Chromospheric evaporation". This was directly observed later on, in blue-shifted lines of hot material.
6. This whole scenario explains the Neupert effect. As the energy from the accelerated particles is converted into the soft X-ray emitting plasma, and it

CHAPTER 1. INTRODUCTION

builds up over time. That explains the soft X-ray being proportional to the time integral of the hard X-ray flux.

This whole scenario is known as the “Standard model of solar flare”. While the standard model is an attempt to explain and unify various kind of differences seen from the neumerous flares we observe, there are several cases where the stnadard model cannot explain the observations. For example, there have been observations of falres where the hard X-ray footpoint do not form. It is proposed that in these cases the plasma in the coronal loops is so dense that the acclerated particle collide enough to thermalize within the flare loops before reaching the Chromosphere, deffusing the energy more evenly within the loop, rather than dumping it at the base of the loops (??). Another flare which previously occured at the same region might explain the denser coronal loops (??).

1.3.4 The energetics of solar flares

With an experience of observing solar flares for more than 150 years, remarkably enough, we have barely started scratching the surface of the complexity involved with the solar flares. The reconfiguring of magnetic structure, which almost always involves complex geometry, making almost all events unique in some sense. After that the released magnetic free energy is transported accross various layers of the sun and converted into various other forms of energy. Consodering how the energy is transformed the magnetic energy of the active region that is released after the reconnection into the reconnection outflow jets, the kinetic energy of escaping particles, the thermal and the kinetic energy of the Chromospheric plasma evaporating, the radiative and conductive losses. In case of the eruptive events, there is the added complexity of the kinetic and potential energy of the CMEs, the enrgy of the shcoks and the kinetic energy of the solar energetic particles.

Inorder to constrain the models of solar eruptions and various nuanced aspects of it, like magnetic reconnection, particle accleration, heating etc. detailed quantitative characterization is absolutely necessary. There have been several studies that have tried to quantify the partition between various subsets of the energies. The questions that are perticularly important are:

- **If an active region can have enough free enrgy to account for the total energy relased in the solar flares and/or CMEs.**
- **What is the energy partition betwen flares and CMEs.**

CHAPTER 1. INTRODUCTION

- If the non-thermal component have enough energy to power up the thermal component.

It is generally well known by now that the active region have enough magnetic free energy to power the flare and CME (??). The partition of energy between the flare and associated CME is much more fuzzy. ? found that the flare and CME have energies of same order of magnitude, while ? concluded the flare dominates the CME in-terms of the energy. However the simple question, whether the non-thermal component of the flares have enough enrgy is still not resolved as even the most recent studies contradict each other in the most puzzling fashion. Here I will discuss the contradictions arising from some of the studies(??????). The details of the studies can be summarized as follows:

Study	No. of flares	GOES class range	Thermal model	Thermal spectrum	Thermal volume	Thermal losses
?	18	A3-B7	Isotherm.	RHESSI	TRACE	X
?	38	C5-X28	Isotherm.	RHESSI	RHESSI	Rad.
?	10	B3-B9	Multitherm.	RHESSI+AIA	RHESSI	Rad.
??	24	C3-X17	Isotherm.	RHESSI+GOES	RHESSI	Rad.,Cond.
?	188	M1-X7	Multitherm.	AIA	AIA	Rad.

Table 1.1:: The details of the studies.

1.4 Motivation

1.5 Outline of Thesis

CHAPTER 1. INTRODUCTION

Chapter 2

Existing Solar Observations and techniques

2.1 Introduction

The remarkable technological progress attained in the last few decades has yielded significant benefits in the form of highly advanced imaging, spectroscopic, and polarimetric instruments designed for astronomical observations. These instruments have empowered us with the ability to scrutinize the Sun with exceptional detail. Specifically, the space based observatories have added new avenues of observing sun. Large portions of the electromagnetic spectra is heavily by Earth's atmosphere **[SR: Reference here]**.

2.2 The Aditya-L1

2.3 The Solar Ultraviolet Imaging Telescope

2.3.1 SUIT & Solar Flares

Solar flares are the most powerful magnetic events in the solar system. They are described as a sudden increase in brightness in localized areas on Sun. Within tens of minutes, they can release over 10^{32} erg of energy, which is emitted across the entire electromagnetic spectrum from radio to gamma rays. They can also launch

CHAPTER 2. SOLAR OBSERVATORIES

high energetic particles into the interplanetary medium. Most of the flares occur in magnetic active regions, and the amount of flare energy released is comparable to the free energy stored in the magnetic system. The term "flare" is generally used explicitly for the entire magnetically-driven event's electromagnetic radiation, as it is the most significant fraction of the total energy liberated. The total energy released varies from event to event. It is also known that larger events occur much less frequently than smaller events.

The Solar Ultraviolet Imaging Telescope (SUIT; ??) is one of the seven payloads onboard the Aditya-L1 mission (?) of the Indian Space Research Organization (ISRO). With its 11 science filters (3 broadband and eight narrowband), SUIT will have the capability to probe different heights of solar atmosphere in photosphere and chromosphere to help us understand the various processes that transport mass and energy from one layer to another. SUIT will provide full disk as well as partial disk images of the Sun with a pixel size of 0.7". Through SUIT imaging, we would be able to resolve solar flares spatially on the surface of the Sun, for the first time in near ultra-violet (NUV), which will help us to address the questions regarding their build-up and triggering mechanism. In addition, to measure the spatially resolved solar spectral irradiance within the wavelength range that is central for studying the Chemistry of oxygen and ozone in the Stratosphere of Earth's atmosphere.

It has been shown that the majority of flare energy emerges at the visible and UV wavelength range (?). ? showed that about 77% of the energy is released in the wavelength range > 200 nm, and only ~23% is seen in extreme ultraviolet (EUV) and soft X-ray (SXR), i.e., below 200 nm (???). Although the energy content in hard X-ray (HXR) is a tiny fraction of the total energy budget, they are still crucial in understanding the energization process (?). However, to develop a comprehensive understanding of solar flares, it is mandatory to perform multi-wavelength studies of all kinds of flares. This may have implications on the physics of the origin of solar flares and different physics processes and contribute to the solar spectral irradiance as a function of the solar activity cycle. Although we have been observing Sun and Solar flares in various wavelengths, the spectral energy distribution of the radiated energy from the flares is still very poorly understood. The first solar flares were observed from the ground in the visible domain (??). It is also well known that the flare emission in the visible domain occurs mainly in $H\alpha$ and Ca II lines (???). However, the lesser understood component of the visible and Near Ultra Violet (NUV) emission is the enhancement of the continuum. The study of the white-light (WL) flares has proven to be very difficult because they have a very short duration and low contrast against the background, making their observation from Earth rare and of poor quality. Also, the flares in NUV are not observable from

CHAPTER 2. SOLAR OBSERVATORIES

any ground-based instrumentation as most of the NUV gets absorbed in the upper atmosphere, thus requires space-based observations.

The origin of the WLFs, i.e., the physical process responsible for generating the continuum and its contribution to the overall energy distribution, is still highly uncertain. The question remains whether WLFs are photospheric phenomena due to H^- free-free emission or chromospheric phenomena due to H free-bound emission. The more recent studies further constrain the origin of the WLFs to be Chromospheric phenomena, as it has been shown that the WL and HXR footpoint centroids are cospatial. Similarly, ? constrained the cospatial WL and HXR footpoints within the chromosphere for three flares. With the help of SUIT, we would be able to localize the WL flares and resolve them on various parts of the Solar disk, which along with observations from Interface Region Imaging Telescope (IRIS), Helioseismic and Magnetic Imager (HMI), would help us localize the source of the WL footpoints and also comment on the formation mechanism of the WL itself.

The spectral energy distribution of flares is one of the critical areas of interest in the physics of flares. A complete understanding of this will help us decode the physical processes involved in solar flares and help quantify their effects on solar spectral irradiance. Ideally, it would be essential to observe flares at all wavelengths simultaneously with sufficient spatiotemporal resolution to figure out the spectral energy distribution of flares. Unfortunately, this is generally not the case, and we have to rely on the sporadic observations made using ground-based instruments in the visible domain. As mentioned earlier, the majority of the flare energy is emitted in the NUV and visible domain. ??, performed statistical studies using a large number of flare observations across a wide energy range. They demonstrated, at the peak of the flare, about 70% of the total energy was radiated in the continuum visible and NUV channel as illustrated in 2.1. SUIT would observe and resolve the solar flares within 200-400 nm using 8 NBs and 3 BBs. This, along with IRIS data, would help us comment on the energy distribution of flares of various classes.

Finally, one of the major question of interest is how the Solar flares affect the Spectral Solar Irradiance (SSI) and Total Solar Irradiance (TSI) variability from a short to much longer, Solar Cycle timescale. ?? performed statistical studies using a large number of flare observations across a wide energy range. For this purpose, they used the full Sun observations of Solar flux from Solar and Heliospheric Observatory (SoHO), three visible Solar irradiances from VIRGO/Solar Photometer (SPM) passbands centred on 402 nm, 500 nm, and 862 nm, respectively, from 1996 to 2008. Additionally, they also use the EUV irradiance in the ranges 0.1-50 nm and 26-34 nm measured by SOHO/Solar EUV Monitor (?) and SXR measurements from

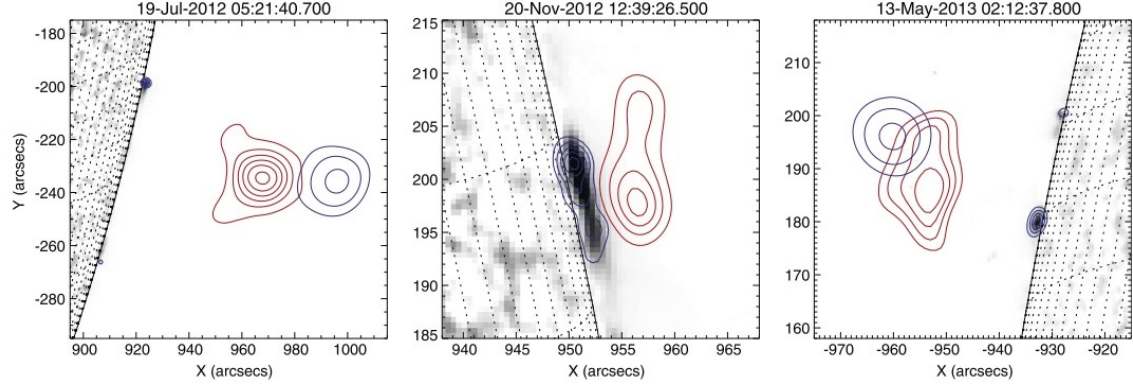


Figure 2.1: X-ray and optical imaging of the three flares at the peak time of the impulsive phase: the images are from HMI with the pre-flare image subtracted. The contours represent RHESSI Clean maps in the thermal (red, 12–15 keV) and non-thermal (blue, 30–80 keV) HXR range (?).

Mean X-ray class	TSI(ergs)	Ratio $\frac{26-34nm}{TSI}$	Ratio $\frac{0-50nm}{TSI}$	Ratio $\frac{0.1-0.8nm}{TSI}$	Ratio $\frac{\text{continuum}}{TSI}$
X3.2	5.9×10^{31}	0.9-0.8%	12-9%	1.2-1%	67%
M9.1	1.6×10^{31}	1.7-0.4%	23-5%	1-0.4%	85%
M4.2	1.3×10^{31}	2.2-0.5%	18-6%	0.6-0.3%	74%
M2.0	5.1×10^{30}	1.7-0.6%	18-6%	0.7-0.4%	69%
C8.7	3.6×10^{30}	1.5-0.5%	16-5%	0.4-0.2%	72%

Table 2.1:: Spectral Energy Distribution from a sample of 2100 flares across various wavelengths(?).

CHAPTER 2. SOLAR OBSERVATORIES

GOES satellites. They showed that stacked TSI variation profiles during solar flares show variation at more than 2 sigma level during the peak flare time, indicating the presence of flare signals in the TSI measurements.

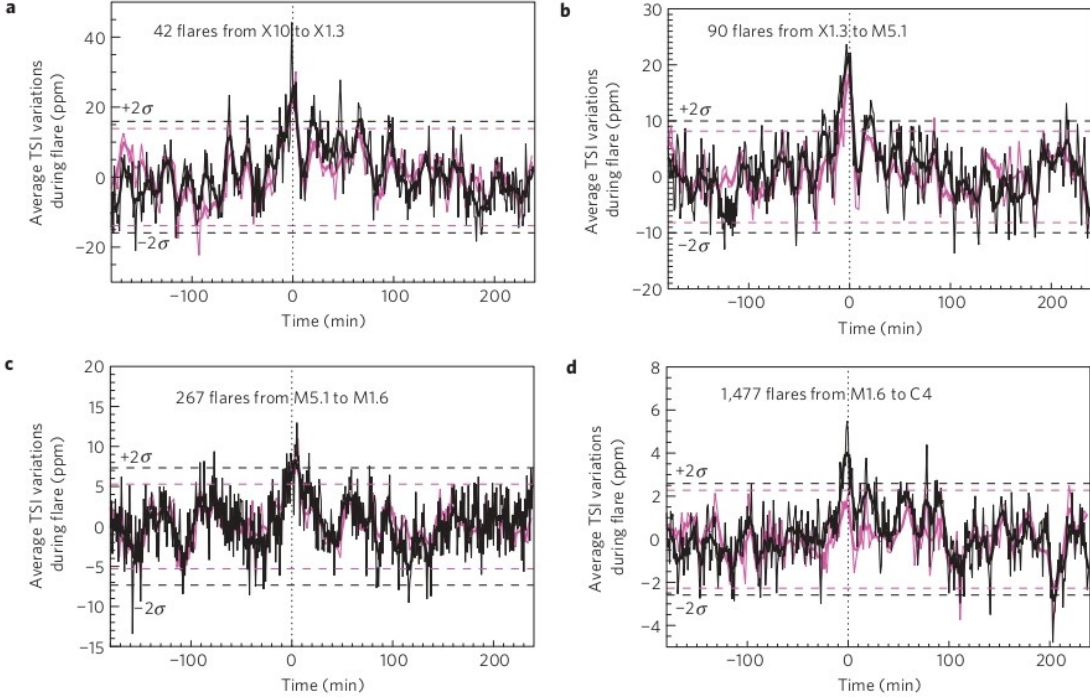


Figure 2.2: Averaged TSI variations during flares. The TSI time-series averages over four exclusive sets of solar flares of decreasing amplitude. The black and pink curves correspond respectively to the TSI measured by the PMOV6 and the DIARAD radiometers. The dashed lines correspond to the 95% confidence levels, while the vertical line denotes the peak time of the flare (?).

This allows us to quantify the solar variability induced by solar flares of various timescales. With the help of SUIT, we would be able to localize the flare locations and study the change in SSI from the local environment in the 11 science filters. This information combined with TSI measurements can allow us to quantify the effect of flares of various energy scales on the TSI variability of the Sun. As, both the TSI and SSI variability directly or indirectly couples with various atmospheric parameters, we can also study the effect the flares have on them. For example, the Earth's atmospheric chemistry and composition respond to any changes in solar UV output in a very nonlinear fashion (?). Since the number of flares also shows a change with solar activity, it is prudent to ask how much flares contribute to the solar spectral irradiance in NUV. This is particularly important because the irradiance in NUV plays a key role in heating the upper and middle layers of the Earth's atmosphere

CHAPTER 2. SOLAR OBSERVATORIES

directly and their coupling with Stratosphere. It also directly influences the middle and lower atmosphere chemistry and composition via the Ozone-Oxygen cycle.

Chapter 3

Intital preparatory analysis for SUIT

*This thesis chapter originally appeared in the literature as
authors, journal reference info*

3.1 Introduction

3.2 Throughput model of SUIT

3.3 Filter Choice for SUIT

3.4 Photometric, Radiometric & Spectral Calibration of SUIT

CHAPTER 3. SUIT PREPARATORY ANALYSIS

Chapter 4

Forward modelling SUIT observations

*This thesis chapter originally appeared in the literature as
authors, journal reference info*

CHAPTER 4. SUIT FORWARD MODEL

Chapter 5

Stellar calibration of SUIT

*This thesis chapter originally appeared in the literature as
authors, journal reference info*

CHAPTER 5. SUIT STELLAR CALIBRATION

Chapter 6

Effects of Solar flares on the local plasma environment from Mg II observations

This thesis chapter originally appeared in the literature as
The Evolution of the Ratio of Mg II Intensities During Solar Flares,
Soumya Roy and Durgesh Tripathi *journal reference info*

6.1 Introduction

Solar flares are the most energetic events on the Sun, where an enormous amount of magnetic free energy is released due to the reconfiguration of the coronal magnetic field. The released energy can cause particle acceleration, heating and flows in the solar atmosphere and a transient enhancement in solar radiative output. It is observed that most of the energy radiated in flares originates from the dense chromosphere (??). Hence, studying the chromospheric lines during flares provides us with diagnostics, which may be important for understanding the physics of solar flares and their effect on the local plasma environment.

The chromosphere emits in various UltraViolet(UV) and optical lines. While many optical lines, e.g., H α , Ca II, are routinely observed from ground-based telescopes, observations in the Mg II resonance lines have been rare in the past. Since the launch of the Interface Region Imaging Spectrograph (IRIS; ?) we have been in the position to monitor these lines regularly with excellent spatial and spectral resolution.

CHAPTER 6. SOLAR FLARE ENERGETICS

The Mg II k and h lines are transitions to the ground state from a finely split pair of upper levels ($3p^2P_{32}$ – $3s^2S_{12}$ and $3p^2P_{12}$ – $3s^2S_{12}$). These transitions create the optically thick lines in the wavelengths 2796.34 Å (Mg II k) and 2803.52 Å (Mg II h). It is suggested that the intensity ratios of these lines can be used to probe the optical depth of the local environment (?).

The integrated intensity of a line transitioning from an upper-level j to a lower-level i , is dependent on the collision strength for that transition Ω_{ij} , which is given by (??),

$$\Omega_{ij} = \frac{8\pi}{\sqrt{3}} \frac{I_H}{\Delta\epsilon_{ij}} g \omega_i f_{ij}$$

Where I_H is the ionization energy of Hydrogen, $\Delta\epsilon_{ij}$ is the threshold energy for the transition, g is the Gaunt factor, ω_i is the statistical weight of the level and f_{ij} is the oscillator strength. In optically thin conditions, the intensity ratio of the k to h line is the ratio of the collision strengths, as the escape probability of photon is unity. The Mg II k and h lines share the same ionization state and originate from a transition to a shared lowered level. As the statistical weight (ω_i) is same in both cases, the line intensity ratio is simply the ratio of the oscillator strengths(f_{ij}). This implies the ratio is 2:1 in optically thin conditions, and lower when the medium is optically thick (??).

In addition, the Mg II k and h lines can be used to estimate the velocity in the middle and upper chromosphere, the chromospheric velocity gradients, the temperature in the middle chromosphere (???). The Mg II triplets in emission can be used to identify heating in the lower chromosphere (?). There have also been multiple studies that have shown a spatial variation of the Mg II line profiles (??). ? showed that the leading edge of the flare ribbon is associated with enhanced broadening and strong central reversal. They interpreted the difference in the profile as a difference in the heating mechanism at the leading edge and bright part of the flare ribbons. ?? showed similar differences between the line profiles and energy input.

Using the observations recorded by the OSO-8 LPSP instrument, (?) studied the evolution of the intensity ratio of Mg II h & k, Ca II h & k and Ly α & β lines. ? showed that the intensity ratio of the Ca II k/h lines increased from 1 to 1.2 during the ascending phase of a flare and returned to 1 during the later phases. The authors interpreted the correlated temporal behavior across various elements as an indication of downward energy propagation. We note that this may suggest a slight decrease in the opacity due to localized heating at the formation height of the Ca II

CHAPTER 6. SOLAR FLARE ENERGETICS

line during the rise phase of the flare.

Here, we study the evolution of the intensities ratios of the Mg II h & k lines during the course of the evolution of three flares, *viz.*, C-class, M-Class and X-class. We focus on the the dependence of line ratios on the underlying magnetic field strength, which to our knowledge has not been explored so far. The rest of the paper is structured as follows. §?? discusses the observations used in this paper. We discuss how we reduce and analyze the data and the results in §??.

CHAPTER 6. SOLAR FLARE ENERGETICS

Chapter 7

Estimating thermal and non-thermal energy partition of Solar Flares

*This thesis chapter originally appeared in the literature as
authors, journal reference info*

CHAPTER 7. SOLAR FLARE ENERGY

Chapter 8

First X-class flare observed from SUIT

*This thesis chapter originally appeared in the literature as
authors, journal reference info*